Elisabetta Comini
Guido Faglia
Giorgio Sberveglieri
Editors

Solid State Gas Sensing

Springer

Solid State Gas Sensing

Elisabetta Comini · Guido Faglia · Giorgio Sberveglieri
Editors

Solid State Gas Sensing

Springer

Editors
Elisabetta Comini
Sensor Laboratory
CNR-INFM and Brescia University
Via Valotti, 9
25133 Brescia
Italy

Guido Faglia
Sensor Laboratory
CNR-INFM and Brescia University
Via Valotti, 9
25133 Brescia
Italy

Giorgio Sberveglieri
Sensor Laboratory
CNR-INFM and Brescia University
Via Valotti, 9
25133 Brescia
Italy

ISBN: 978-0-387-09664-3 e-ISBN: 978-0-387-09665-0
DOI: 10.1007/978-0-387-09665-0

Library of Congress Control Number: 2008929496

Printed on acid-free paper

springer.com

Preface

Gas sensor technology has advanced remarkably during the past few decades and is becoming an essential technology. Many gas sensors are now commercially available and researchers are making efforts, thanks to pioneering novel ideas, to develop next-generation gas sensors, having all the necessary requirements, such as small size, low production costs and power consumption.

This book covers all gas sensor topics, a research field with an increasing interest in the last few years due to the demands of reliable, inexpensive and portable systems for environmental monitoring, indoor air quality, food quality control and many other applications. The goal of this book is to provide a critical assessment of the new trends in the gas sensor field, by describing the working principle and the applications related to the different types of sensors and paying attention to the recent impact of nanotechnology on the field.

Nanotechnology is a new field that will dramatically change solid-state gas sensing. In the last few decades, the study of one-dimensional (1D) materials has become a primary focus in nanoscience and nanotechnology. With reduction in size, novel electrical, mechanical, chemical and optical properties have been introduced, which are largely believed to be the result of surface and quantum confinement effects. For example, nanowire-like structures are the ideal system for studying the transport process in one-dimensionally (1D) confined objects, which are of benefit not only for understanding the fundamental phenomena in low dimensional systems but also for developing new generation nanodevices and gas sensors with high performances.

The first chapter is devoted to micro-fabrication for gas sensors. Following chapters deal with the subject on the base of the transduction principle as electrical, permittivity, field effect, electrochemical, optical, thermometric and mass (both quartz and cantilever types) based.

The book is characterized by a methodical and thorough treatment of the subject matters. The chapters are logically related, and each has its own introduction and bibliography, in order to make it accessible to any reader notwithstanding his background on related subjects.

Since the last years have seen an enormous amount of activity in the field of gas sensor systems, this book represents a valuable and accessible guide and reference for researchers with up-to-date examples and state-of-the-art results.

Italy
May 2008

Elisabetta Comini
Guido Faglia
Giorgio Sberveglieri

Contents

Contributors

István Bársony
Research Institute for Technical Physics and Materials Science – MFA
Hungarian Academy of Sciences, Budapest, Hungary

Ilaria Cacciari
CNR, "Nello Carrara" Institute of Applied Physics (IFAC), 50019 Sesto
Fiorentino, Italy

Elisabetta Comini
Sensor Laboratory, CNR-INFM and Brescia University, Via Valotti, 9, 25133
Brescia, Italy, comini@ing.unibs.it

Csaba Dücső
Research Institute for Technical Physics and Materials Science - MFA
Hungarian Academy of Sciences, Budapest, Hungary

Perumal Elumalai
Art, Science and Technology Center for Cooperative Research, Kyushu
University, Kasuga-shi, Fukuoka, 816-8580, Japan

Guido Faglia
Sensor Laboratory, CNR-INFM and Brescia University, Via Valotti, 9, 25133
Brescia, Italy, guido.faglia@ing.unibs.it

Péter Fürjes
Research Institute for Technical Physics and Materials Science - MFA
Hungarian Academy of Sciences, Budapest, Hungary

Andreas Helwig
EADS Innovation Works, D81663 München, Germany

Samuel J. Ippolito
RMIT University, Department of Applied Chemistry, Melbourne, Victoria
Australia, sipp@ieee.org

Hans Peter Lang
National Center of Competence for Research in Nanoscale Science, Institute of Physics of the University of Basel, Klingelbergstrasse 82, 4056 Basel Switzerland, Hans-Peter.Lang@unibas.ch

Norio Miura
Art, Science and Technology Center for Cooperative Research, Kyushu University, Kasuga-shi, Fukuoka, 816-8580, Japan
miurano@astec.kyushu-u.ac.jp

Gerhard Müller
EADS Innovation Works, D81663 München, Germany
Gerhard.mueller@eads.net

Lars Ojamäe
Department of Physics, Chemistry and Biology, Linköping University
SE-581 83 Linköping, Sweden, lars@ifm.liu.se

Vladimir V. Plashnitsa
Art, Science and Technology Center for Cooperative Research, Kyushu University, Kasuga-shi, Fukuoka, 816-8580, Japan

David A. Powell
Australian National University, Research School of Physical Sciences and Engineering, Canberra, ACT, Australia, david.powell@ieee.org

Giancarlo C. Righini
CNR, "Nello Carrara" Institute of Applied Physics (IFAC), 50019 Sesto Fiorentino, Italy; CNR, Department of Materials and Devices, 00185 Roma, Italy
g.c.righini@ifac.cnr.it

Yoshihiko Sadaoka
Department of Materials Science and Biotechnology, Graduate School of Science and Engineering, Ehime University, Matsuyama 790-8577, Japan
sadaoka@eng.ehime-u.ac.jp

Giorgio Sberveglieri
Sensor Laboratory, CNR-INFM and Brescia University, Via Valotti, 9, 25133 Brescia, Italy, sbervegl@ing.unibs.it

Olaf Schulz
EADS Innovation Works, D81663 München, Germany

Magnus Skoglundh
Competence Centre for Catalysis, Chalmers University of Technology
SE-412 96 Göteborg, Sweden, skoglund@chalmers.se

Jan Spannhake

EADS Innovation Works, D81663 München, Germany

Anita Lloyd Spetz
Department of Physics, Chemistry and Biology, Linköping University
SE-581 83 Linköping, Sweden, spetz@ifm.liu.se

Adrian Trinchi
CSIRO Division of Materials Science and Engineering, Melbourne, Victoria
Australia, avt@ieee.org

Taro Ueda
Interdisciplinary Graduate School of Engineering Sciences, Kyushu University
Kasuga-shi, Fukuoka, 816-8580, Japan

Masahiro Utiyama
National Institute for Environmental Studies, Tsukuba-shi, Ibaraki, 305-8506
Japan

Ryotaro Wama
Interdisciplinary Graduate School of Engineering Sciences, Kyushu University
Kasuga-shi, Fukuoka, 816-8580, Japan

Wojtek Wlodarski
RMIT University, School of Electrical and Computer Engineering, Melbourne
Victoria, Australia, ww@rmit.edu.au

Chapter 1
Micro-Fabrication of Gas Sensors

Jan Spannhake, Andreas Helwig, Olaf Schulz, and Gerhard Müller

1.1 Introduction

Gas sensors are increasingly used in the growing markets of automotive [1, 2, 3], aerospace [2, 3, 4, 5, 6, 7], and logistic [8, 9, 10] applications. Within these domains, gas sensors play important roles in providing comfort and safety or in enabling process control or smart maintenance functionalities. Future important markets are likely to emerge in the fields of safety and security [11]. With regard to the sensitivity and selectivity of gas detection these various applications require very different levels of sensor performance. Very often the different applications also impose highly varying price, size, weight, and power consumption constraints on an acceptable sensor solution. In practice, therefore, a whole range of different gas sensors and gas-sensing principles need to be employed [8, 9, 10, 11]. Although the sensitivity of gas detection is not normally a major concern, selectivity is much harder to attain. Usually selectivity is obtained at the expense of an increased system complexity [11]. Depending on the degree of selectivity required, gas sensors can take the form of simple low-cost solid-state devices with broadband sensitivity or the form of desktop analytical instruments in case high selectivity is required.

In the field of low-cost solid-state gas sensors, metal oxide sensors have found widespread commercial application [12, 13, 14, 15]. Such sensors consist of gas-sensitive metal oxide (MOX) materials screen-printed onto ceramic heater substrates. To date such sensors are being produced in quantities of several millions per year, mainly for applications in the automotive and domestic markets. In the automotive industry, MOX gas sensors are used to control the air ventilation flaps in an attempt at keeping toxic air contaminants or highly odorous gases to a minimum in the car interior [3]. In the domestic market, MOX gas sensors are being used to detect natural gas leaks and to set off alarms before any explosive air–gas mixture might have developed.

G. Müller
EADS Innovation Works, D81663 München, Germany
e-mail: Gerhard.mueller@eads.net

E. Comini et al. (eds.), *Solid State Gas Sensing*,
DOI: 10.1007/978-0-387-09665-0_1,

Such inexpensive gas sensors provide high sensitivity to a wide variety of gases. However, they have also become ill-famed for their cross-sensitivity and the resulting high level of false alarms. Considering their high sensitivity and low complexity, considerable attempts have been undertaken to improve the selectivity of MOX gas sensors. In order to achieve this, many different kinds of MOX materials have been studied [15]. Rather than arriving at materials with narrow cross-sensitivity profiles, a range of materials with broad, but distinctly different cross-sensitivity profiles has evolved. Attempts at arriving at higher selectivity with MOX gas sensors therefore have concentrated on forming arrays of several MOX gas sensors with different cross-sensitivity profiles [12, 16, 17, 18, 19, 20]. In this case pattern recognition techniques are applied to the multi-sensor output to arrive at an acceptable level of gas discrimination. It has become popular to refer to such arrays as "electronic nose" devices [18]. Application areas of electronic nose devices range from the food industry up to supply chain monitoring in the automotive industry.

High-performance gas sensors, on the other hand, usually employ spectroscopic principles such as optical absorption spectrometry [21], gas chromatography [22] or ion mobility spectrometry [23]. Examples of optical spectrometers are dispersive and non-dispersive infrared (IR) absorption gas detectors [16, 24]. Such devices are selective in that they identify the molecules of interest by their specific molecular vibration modes. IR-based devices therefore produce fewer false alarms than MOX-based gas detectors in similar applications. However, they cannot usually compete with the superior gas sensitivity of MOX gas sensors. The range of applications of IR-based gas sensors is therefore limited to a certain range of air quality monitoring and leak detection applications. In case higher sensitivity is required – as in security applications – it has become popular to employ chromatographic and/or ionization based detection principles [23]. This latter range of devices allows tiny traces of explosives, illicit drugs and other contraband materials to be detected in a huge background of less interesting air constituents or commonly occurring air contaminants.

In the past two decades micro-electro-mechanical systems (MEMS) miniaturization techniques have started to penetrate all these various fields of gas-sensing technologies. Examples of MEMS-based sensing devices now range from low-power MOX gas sensors [19, 20, 25, 26] up to miniature mass spectrometers including on-chip vacuum generation [27]. The driving force in all these miniaturization attempts is arriving at small-size low-cost devices, either for the use in handheld instruments or as miniaturized low-power consumption devices in distributed and bus-connected sensor networks. In all these applications MEMS batch fabrication technologies are not only interesting because of their miniaturization potential but also because of their potential of providing high performance at low cost in mass production scenarios.

In a limited size review, like the present, it is impossible to do justice to the whole range of MEMS developments that have been undertaken so far. In the following we will therefore concentrate on development work carried out in

the author's laboratory. In this work the focus has been building up a MEMS toolkit [28] around thermal microstructures to allow miniaturized gas-sensing systems to be set-up in a flexible manner. Using this kit, both MOX and IR-based gas-sensing microsystems have been realized and tested in various application scenarios. In the following the individual components in this toolkit will be described and several examples of micro-sensor systems will be pointed out. Last-not-least, industrialization issues are discussed that need to be dealt with to introduce MEMS gas-sensing systems into high-tech end-user markets.

1.2 Gas Sensors and MEMS Miniaturization Techniques

During the past five decades, silicon microelectronics technology has been the driver for the so-called microelectronics revolution. During that time electronic micro-miniaturization techniques have smoothly developed into a highly developed top-down nanotechnology with minimum feature sizes now approaching the 45 nm region [29, 30]. Later on the silicon base technology was extended to allow three-dimensional mechanical structures to be formed out of mono-crystalline silicon and/or silicon-compatible thin-film materials. This latter field is now generally referred to as MEMS [31, 32, 33]. In this latter form the silicon technology has also started to contribute to the evolution of chemical sensors and chemical sensor systems [25, 26]. Before we enter into a detailed discussion of MEMS gas sensors and MEMS gas-sensing systems, we take a brief look at the silicon technology and the silicon semiconductor material itself to see how both can contribute to the development of micro-gas-sensors and micro-gas-sensor systems.

1.2.1 Silicon as a Sensor Material

Whereas mono-crystalline silicon is widely recognized as the base material for the microelectronics industry, it is also well-known that silicon supports a variety of solid-state effects that make it interesting as a sensor material [17]. Transduction effects that are useful for the fabrication of micro-sensors serving the five main signal domains are indicated in Fig. 1.1.

Making use of these effects, a wide variety of sensor devices can be produced, which, in addition to the very sensing function, also contain important down-stream electronic functionalities such as preamplification and temperature compensation. The second important feature of silicon sensors is related to the fact that both the sensing and the electronic functions can be realized using a common set of processing steps, which can all be carried out on wafer-scale, i.e., in a batch process, which allows large economic benefits in mass production.

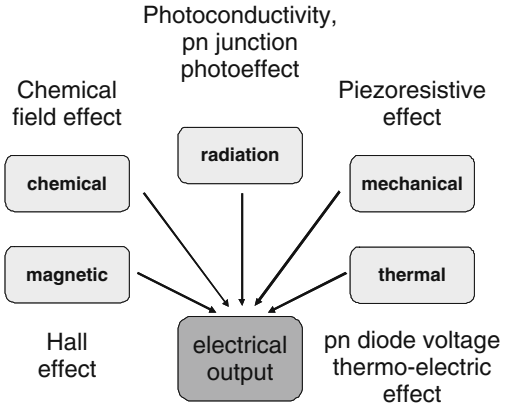

Fig. 1.1 Sensor signal domains and silicon solid-state effects that allow non-electrical input signals to be transformed into an electrical output signal using silicon sensor devices

Considering Fig. 1.1, however, it is also relevant to note that silicon as a semiconductor material is only of limited use for the fabrication of chemical sensors in general and for gas sensors in particular. Examples of silicon-based chemical sensors are pH- and ion-sensitive field-effect transistors and catalytic-gate MOS (metal oxide semiconductor) gas sensors. Whereas the first kind of device was introduced by Bergveld et al. [34], the latter was first described by the Lundström group [35, 36, 37]. In the meantime, all these devices have been developed to a considerable degree of sophistication. The functioning of both kinds of devices is based on the interaction of the analyte ion or analyte gas species with SiO_2 surfaces, i.e., with the surface of those oxide layers that naturally form on silicon surfaces. A severe constraint of catalytic-gate MOS gas sensors is that, in the normal operating temperature range of silicon devices, such sensors are almost completely selective to H_2. They therefore do not provide a sufficiently generic approach towards micro-gas-sensors. The field of semiconductor gas sensors, therefore, has very much remained a field of specialized transducer materials such as MOXs [15, 38], polymers [39], and other kinds of gas-sensitive materials [40].

1.2.2 Thermal Sensors and Actuators

A breakthrough in the field of silicon-based gas sensors occurred once silicon-based MEMS technologies became available [31, 32, 33]. Evolving out of the traditional microelectronic silicon processing technology, MEMS technology includes additional processing steps such as bulk- and surface-micromachining processes as well as silicon and glass wafer bonding techniques. In this way it has become possible to produce miniaturized devices, which combine mechanical, electrical, and thermal functionalities within a single piece of silicon. In addition, the portfolio of MEMS processes also includes an increasing variety of silicon-compatible functional materials to enable sensor and actuator

functionalities that are impossible to realize using the silicon base material itself. Important representatives of such functional materials are thin- and thick-film gas-sensitive layers.

Whereas MEMS fabrication techniques have first made a major impact in the field of mechanical sensors such as pressure transducers, accelerometers, angular rate sensors, and so forth [17, 41], MEMS micro-miniaturization techniques soon thereafter have started to contribute to the development of miniaturized gas sensors and gas-sensing devices as well [25, 26]. In this latter context, the capability of MEMS technologies to arrive at thermal microstructures has proven to be most useful. Such microstructures are the basic building blocks in thermal sensor and actuator devices [36].

Thermal sensors (Fig. 1.2a) represent a special class of sensors that convert the input signals of interest into an intermediate thermal signal – usually a temperature change – that is then electrically detected by performing a temperature measurement. Figure 1.2b further shows that by inverting the direction of the energy flow in a thermal transducer, thermal sensors can be converted into thermal actuators. In this latter case the non-electrical output energy form is generated by dissipating electrical energy. The thermal energy in turn is converted into the output energy form.

The usefulness of thermal microstructures is revealed if we consider some specific cases. Considering the case of IR gas detection first, we note that here a thermal actuator may be used to produce the thermal IR radiation that may be absorbed by the analyte gas molecules and that the transmitted IR radiation in turn may then be detected by a bolometer or a thermopile, i.e., a thermal IR detector. Thermal sensors and actuators therefore, form integral parts of various kinds of infrared gas-sensing microsystems [16, 24, 42]. Considering other kinds of gas-sensing technologies, thermal microstructures often play the dual

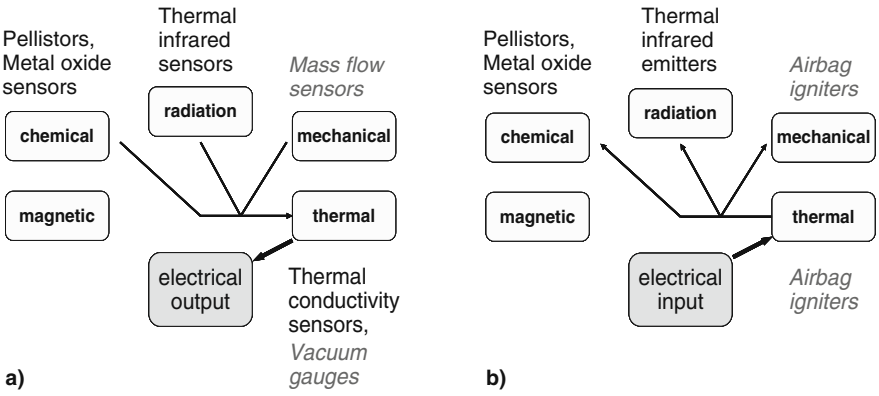

Fig. 1.2 Functional principle of thermal sensors (**a**) and of thermal actuators (**b**). For the sake of illustration some typical application examples are mentioned. Non-gas-sensing applications with mass production potential are indicated by italic letters

role of a sensor and an actuator within one and the same device. Such a situation, for instance, arises in the case of thermal conductivity gas sensors [43]. Such sensors consist of a heated membrane, which is cooled by the ambient atmosphere. As an actuator this microstructure produces the heat that is carried away by the molecules in the ambient atmosphere. As a sensor this microstructure senses the heat that is being carried away and thus provides information concerning the molecular composition of the ambient atmosphere. This dual role can also be observed in catalytic gas sensors, i.e., pellistors [44]. Such devices first produce the heat that is required to initiate chemical reactions of the analyte molecules at a catalytically active surface and secondly they detect the amounts of heat that are generated as the analyte molecules are being burnt at the sensor surface. Once heated to the reaction threshold, micro-heaters may also enable conductance changes in MOX materials [45, 46, 47, 48] that had been deposited onto such micro-heaters. Thermal sensors and actuators also do play a role in non-gas-sensing applications as for instance in the automotive industry. Important mass-driver applications are thermal mass-flow sensors and air-bag igniters.

These examples show that thermal microstructures can be used in a variety of ways to arrive at micro-gas-sensors. Furthermore there is a potential that their production can be aligned with the production of non-gas-sensing devices to arrive at production lots that are sufficiently large to benefit from the MEMS mass production capabilities. Before discussing specific application examples, we still need to consider some general architectural and technological details relevant to thermal microstructures.

1.2.3 Thermal Microstructures

In order to operate thermal sensors and actuators efficiently, it is necessary to produce maximum temperature changes from a minimum amount of input energy. Thermal microstructures live up to this requirement by combining small heat capacitance with a high degree of thermal insulation. Architectures that have been widely used to realize thermal microstructures are summarized in Fig. 1.3.

A first way of obtaining active device structures with a low heat capacitance and a high degree of thermal insulation is building thin-film stacks on silicon wafers with predeposited dielectric passivation layers. Thermal insulation of the active device structures is attained by removing the silicon substrate underneath the active devices. To this end, anisotropic silicon etching techniques have been extensively used [45, 49, 50]. This first approach is illustrated in the top row of Fig. 1.3 and a micro-heater element ready for deposition of a thin-film MOX gas-sensing layer is shown on the right as a device demonstrator.

Standard materials for forming such suspended membrane structures are silicon dioxide (SiO_2) and silicon nitride (Si_3N_4) – either in the form of layer

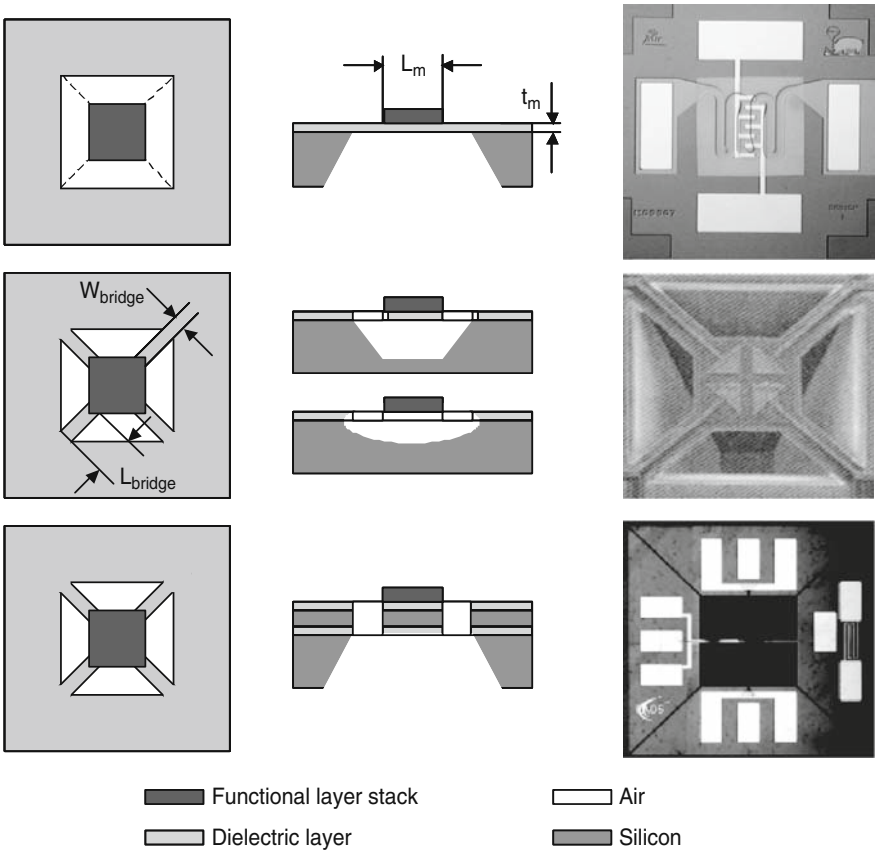

Fig. 1.3 Principle architectures of thermal microstructures. *Left row*: schematics top view; *middle row*: schematics cross-section; *right row*: realized device demonstrators. The active area in the membrane centre usually contains a thin-film stack consisting of a Pt meander that can serve both as a heater and temperature sensing element, a dielectric passivation layer and additional functional layers that depend on the very device application. Geometrical parameters that critically determine the device performance are indicated in the schematics

stacks or in the form of thin-film alloys – to arrive at a small level of tensile mechanical stress inside the suspended membrane. Forming a Pt meander on top of such a membrane, the structure can be used both as a thermal sensor and an actuator device. This double function is enabled by the fact that Pt exhibits a positive and almost linear temperature coefficient of resistivity (TCR). Pt meanders, therefore can serve both as active heating as well as a passive temperature sensing elements. In order to avoid catalytic interactions with the heated Pt meander, the meander is coated with a thin, chemically inert layer of SiO_2. Very often, such passivation layers form the substrate for further functional layers that may be required to arrive at a particular sensor or actuator function. In the demonstrator case shown, one can recognize an interdigital

contact layer. Deposition of an additional MOX layer turns the device into a low-power-consumption MOX gas sensor. Other layer combinations can turn the device into a heat conductivity sensor, a pellistor, or a bolometer.

A second approach to thermal microstructures is shown in the middle row of Fig. 1.3. There front-side etching of the silicon substrates is used to define the thermally insulated membrane structures. As this approach requires accessibility of the silicon substrate through the top-surface dielectric membrane during the device processing, spider-like membrane geometries evolve as shown in the middle column. Using front-side etching, device dimensions can be reduced to the smallest necessary minimum. Due to the extremely small heat capacitance and the exceptionally good thermal insulation provided by the four dielectric membrane suspensions, heater devices with extraordinarily low electrical power consumption and very fast thermal response times can be obtained. This latter approach has been intensively employed by the NIST (National Institute of Standards and Technology) group in their research on MOX gas sensors and sensor arrays [46, 47, 48]. Whereas the NIST group used anisotropic silicon etching [49, 50] to generate an etch trough underneath the dielectric membrane structure (see the device demonstrator in the middle row of Fig. 1.3), other groups have employed porous silicon sacrificial layer etching [51, 52]. As porous silicon etching is an isotropic process, some underetching takes place that laterally extends the air cushion underneath the membrane structure beyond its mask-defined limitations.

In the past several years our own research has concentrated on silicon-membrane devices [28, 49, 50, 51]. In this latter case the membrane structures and their mechanical suspensions consist of mono-crystalline silicon. An easy and efficient way of producing such devices is employing silicon-on-insulator (SOI) techniques. This latter approach is schematically illustrated in the bottom row of Fig. 1.3. A more detailed cross-section through such a device is shown in Fig. 1.4 together with some clues concerning their technological realization.

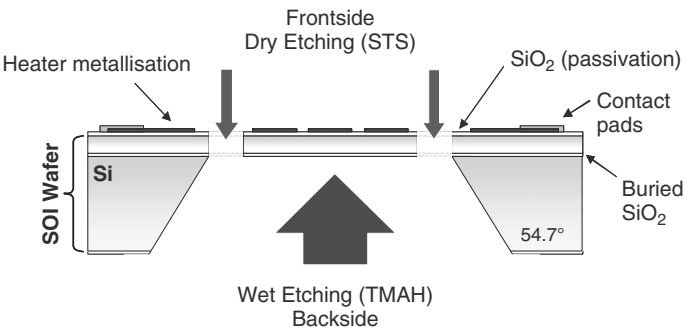

Fig. 1.4 Cross-section through a SOI-based micro-heater device. The membrane structure consists of a thin mono-crystalline silicon layer that is thermally, electrically and mechanically separated from a thick supporting handle wafer

Because the thermal conductivity of bulk silicon is roughly one hundred times higher than that of SiO_2 or Si_3N_4, ultra-low-power-consumption devices cannot be made with this kind of SOI technology. The disadvantage of high thermal conductivity of the silicon membrane material, however, is offset by a number of advantages:

(i) Superior mechanical stability with regard to dielectric membranes [28],
(ii) Integration of active semiconductor devices into the membrane material [53, 54, 55, 56],
(iii) Direct resistance heating of the membrane material [50, 53],
(iv) Enhanced high-temperature stability (T$\sim$1000°C) due to the reduced electro-migration in semiconductor as compared to noble metal heaters [50, 57],
(v) Usefulness of the SOI base technology also for other kinds of membrane-type devices such as silicon microphones [58, 59, 60] or flexural plate wave devices [61], which are all of considerable interest in the field of chemical sensors [62].

Quantitatively the performance of the above microstructures depends on material properties, device dimensions and the conditions of device operation. An efficient tool for analyzing the gross performance of such devices is the method of thermal equivalent circuits. Mathematical details concerning this approach have been presented elsewhere [63, 64]. Qualitatively the idea behind this approach is illustrated by the thermal equivalent circuits presented in Fig. 1.5.

In this equivalent circuit it is assumed that heated membrane devices, like the ones shown in Figs. 1.3, can be modeled assuming a homogeneously heated membrane center, heated to a temperature $T_m > T_a$. For simplicity it is further assumed that heat is not generated in the periphery of the membrane that

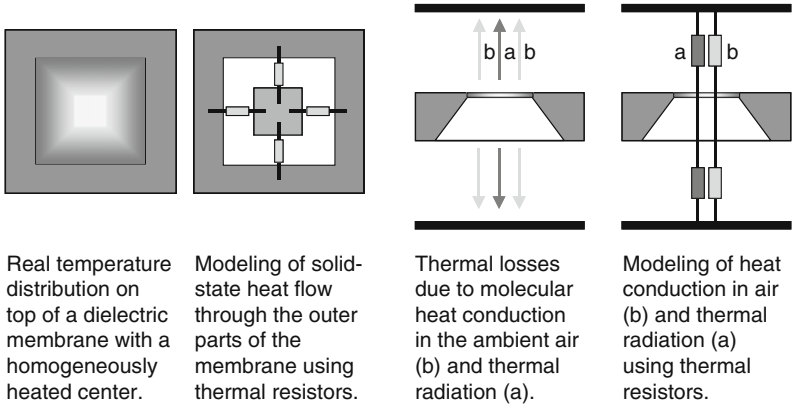

Fig. 1.5 Thermal equivalent circuit describing the flow of heat from a homogeneously heated membrane towards its neighboring heat sinks

bridges the heated membrane center with the cold silicon rim, maintained at the ambient temperature T_a. Heat conduction from this membrane center can then occur via three independent processes: (i) solid-state heat conduction through the membrane, (ii) heat conduction (convection) through the ambient air, and (iii) heat radiation. Each of these processes can be associated with equivalent thermal resistors whose magnitude depends on the temperature difference ($T_m - T_a$), as well as on the thermal and geometrical properties of the heat transporting medium that bridges the gap between the heated membrane center and its cold surroundings [65, 66]. As in electrical circuits, the overall thermal resistance R_{th} of the membrane structure arises from the parallel combination of the individual thermal resistances. Further, using the equivalent of Ohm's law for thermal equivalent circuits the temperature of the membrane center can be obtained as a function of the thermal power that is input into the membrane center:

$$T_m - T_a = R_{th}(T_m - T_a) \cdot P_{in}. \tag{1.1}$$

This latter result shows that a high thermal resistance minimizes the input power P_{in} for attaining a certain membrane temperature T_m. Furthermore this result shows that the actual value of T_m depends on T_a, i.e., on the ambient temperature in which the micro-heater is being operated in. The temperature baseline value of T_a therefore corresponds to the zero-potential baseline in the equivalent electrical circuit.

Neglecting heat conduction, convection and thermal radiation, which can be the dominant thermal losses from a heated membrane, the thermal response time τ_{th} of the microstructure can easily be estimated. This latter time constant measures the rate with which the temperature of the membrane centre can follow changes in the thermal input power P_{in}. Again, as in the electrical case, this time constant is given by the product of the thermal resistance R_{th} and the thermal capacitance C_{th} of the microstructure:

$$R_{th} = \left(\frac{1}{4}\right) \cdot \left(\frac{1}{\lambda_{solid}}\right) \cdot \left(\frac{L_{bridge}}{t_m \cdot W_{bridge}}\right) \tag{1.2a}$$

λ_{solid} : thermal conductivity of membrane material
L_{bridge} : length of non-heated bridging rim of membrane
W_{bridge}: effective width of non-heated bridging rim of membrane
t_m : thickness of membrane

The factor of ¼ derives from the fact that heat is dissipated into four bridging resistors at all four sides of the heated membrane center.

$$C_{th} = \rho_{solid} \cdot C_{P\_solid} \cdot L_m^2 \cdot t_m \tag{1.2b}$$

ρ_{solid} : mass density of membrane material
C_{p_solid}: heat capacity at constant pressure of membrane material.

With the latter two formulas, the thermal time constant can be obtained as a function of the thermal properties of the membrane material and the geometrical dimensions of the membrane structure:

$$\tau_{th} = \left(\frac{\rho_{solid} \cdot C_{p\_solid}}{\lambda_{solid}}\right) \cdot \left(\frac{L_{bridge}}{W_{bridge}}\right) \cdot \left(L_m^2\right) \tag{1.3}$$

Inserting typical values, time constants in the range of milliseconds are revealed. On the other hand, this latter formula also reveals a trade-off. Whereas small heated areas (L_m^2) clearly minimize τ_{th}, there is a conflict when we simultaneously want to obtain good insulation and a small time constant: whereas forming long and narrow bridges yields large thermal resistances and good thermal insulation, the reduced heat flow through such suspensions also leads to long time constants. Similar considerations also apply to the heat conductivity of the membrane materials. This conflict is the thermal analog of the well-known gain–bandwidth limitation in conventional electrical engineering.

1.3 Specific Sensor Examples

In this chapter we should like to discuss how the base structures described above can be used to realize actual device functionalities. The examples discussed include heat conductivity sensors, MOX and field-effect gas sensors as well as thermal infrared emitters. This range of devices is far from being exhaustive. However, it is large enough to demonstrate some of the main features and applications of thermal microstructures.

1.3.1 Heat Conductivity Sensors

Among the thermal microstructures shown in Fig. 1.3 those with dielectric membranes feature the highest degree of thermal insulation and the smallest thermal mass. The high thermal insulation results from the very low heat conductivity of the membrane materials and the low thermal mass from the small thickness of the dielectric membranes ($t_m \sim 0.2$ μm). Operating such a device in ambient air, the membrane center can be heated to about 400°C at the expense of an electrical power input of about 20 mW into the Pt heater meander. Operating this same device in vacuum, the power consumption is reduced to about 2–3 mW. The individual contributions to the heat loss as estimated from the above thermal resistor model are shown as a function of the membrane temperature in Fig. 1.6a. Figure 1.6b shows how the thermal time constant of this same device varies as the temperature of the membrane center is raised.

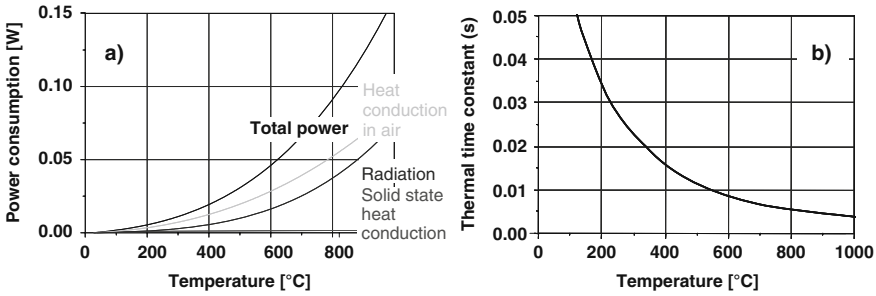

Fig. 1.6 **a**) Calculated heating power consumption of the dielectric-membrane-type device shown in the top row of Fig. 1.3. The individual contributions due to dissipation into solid-state heat conduction, heat transport in air and thermal radiation are indicated; (**b**) thermal time constant as a function of the membrane temperature. The time constant drops with increasing membrane temperature due to the increasing thermal losses due to heat conduction in air and due to thermal radiation

These latter data vividly demonstrate that dielectric-membrane-type heaters make very low-power-consumption and fast-responding devices whose power dissipation is largely determined by heat conduction processes in the ambient air. As a result, the main application of such microstructures to date is in thermal mass flow sensors, which regulate the air intake into car engines [43, 67, 68]. There the convective cooling of flowing air determines the electrical power consumption of the device and, due to their small thermal mass; such devices can follow changes in the air mass flow with single-cylinder resolution. This kind of a non-gas-sensing application, in fact, is a very useful MEMS mass driver application, on which a variety of architecturally related MEMS gas-sensing devices can be based.

In order to operate dielectric-membrane-type micro-heaters as gas sensors, the heaters need to be operated in stationary air. This can be achieved by a packaging as indicated in Fig. 1.7. Very often the access holes in such packages are additionally closed with porous seals that prevent air flows across the heated membrane but allow analyte molecules in the ambient air to diffuse into the sensor package.

In order to see how such as sensor can be used to obtain information about the ambient gas atmosphere, we consider the formula for the heat conductivity λ_{air} of an ideal gas [64, 69]:

$$\lambda_{air}(P, L_c, M_{rel}, T) = \frac{5}{3} \cdot \left(\frac{2 \cdot k_B^3 \cdot T}{\pi \cdot M_{rel} \cdot M_0 \cdot \sigma_s} \right) \cdot \left(\frac{P}{P + P_c} \right) \tag{1.4a}$$

$$P_c = \frac{k_B \cdot T}{\sigma_s \cdot L_c} \tag{1.4b}$$

k_B Boltzmann constant
T air temperature

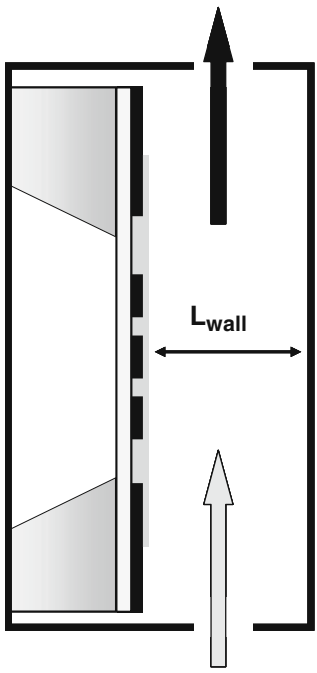

Fig. 1.7 Principle architecture of a heat conductivity sensor. A heated membrane is enclosed in a package with the membrane at a distance L_{wall}. At normal ambient pressure it can be used to detect the presence of combustible gases (H_2, CH_4) in air. At low pressures, in which the mean free path is constrained by L_{wall}, it can be used to measure the vacuum pressure. *Upright positioning* of the sensor accelerates the exchange of air inside the package by thermal convection

P	air pressure
M_{rel}	average molecular mass in atomic mass units
M_0	atomic mass unit (amu)
σ_s	molecular collision cross-section

Here, P_c is a pressure parameter that characterizes geometrically constrained situations, characterized by a critical length L_c. Such situations arise, whenever the molecular mean free path becomes comparable to the geometrical dimensions of the device or its packaging. In Fig. 1.8 the above formula has been evaluated for the packaging situation indicated in Fig. 1.7. There it has been assumed that the motion of the air molecules is confined to the depth of a typical etch trough inside a thermal microstructure, i.e. $L_c = L_{wall} \sim 300$ μm. As revealed from Fig. 1.8 this constraint becomes relevant when the air pressure P is reduced to about 100 Pa, i.e., to about one thousandth of the normal air pressure. Above this pressure the heat conductivity is independent of P but dependent on the average molecular mass (Fig. 1.8a) and on the gas temperature (Fig. 1.8b). Below about 10 Pa, the heat conductivity becomes linearly dependent on P.

The above results can be used in two ways: in the range of normal ambient pressures the dependence of the average molecular mass can be used to detect gases in air whose molecular mass differs from the average molecular mass of air [43]. In the low-pressure range, heated membrane devices can be used to measure the pressure inside vacuum vessels [70].

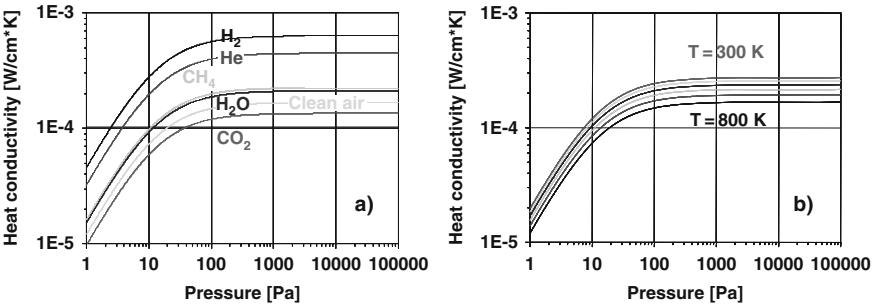

Fig. 1.8 (**a**) Geometrically constrained heat conductivity of clean air at T = 300 K as a function of pressure. Data for H_2, He, CH_4, H_2O, and CO_2 are shown for comparison; (**b**) geometrically constrained heat conductivity of clean air ($M_{rel} = 28.8$) as a function of pressure. Parameter: ambient air temperature

Turning to the gas-sensing application first we note that clean air consists of about 80% N_2 ($M_{rel} = 28$) and 20% O_2 ($M_{rel} = 32$); the average molecular mass of clean air thus turns out to be $M_{rel} \sim 28.8$. Reference to the data of Fig. 1.8a shows that those gases with molecular masses lighter than this should easily be detectable. In this class of gases we find combustible gases such as H_2 and CH_4, i.e., combustible gases that represent safety hazards when their concentration exceeds their lower explosive limits (LEL) of about 4% in air. For detection a heated membrane device is used as in Fig. 1.7 but with the gas inlet and outlet ports being closed by porous membranes. This porous sealing allows for a diffusive gas exchange but it does not allow an ignition process to initiate should the LEL concentration be exceeded. For detection the membrane device is heated above the ambient temperature and kept constant by an electronic control circuit. With this kind of control being established and gases of low molecular weight entering the sensor package, more electrical power needs to be fed into the membrane heater to maintain a constant surface temperature. This excess power consequently can be used as a sensor output signal. The data in Fig. 1.9a show that in this way H_2 can be detected in concentrations far below the LEL of H_2 of 4% or 40,000 ppm. A likely application scenario in the near future will be H_2 driven cars, where safety requires all components of the power train to be monitored for H_2 leakages.

The data of Fig. 1.9b point out a problem that is commonly encountered in the field of chemical sensors, i.e., cross-sensitivity. It shows that heat conductivity sensors not only detect H_2 but also a range of other gases provided two conditions are met: (i) the gas concentration needs to exceed the minimum detectable concentration of about 1000 ppm and the gases need to have a molecular mass that is different from the average mass of clean air, i.e., $M_{rel} \sim 28.8$. Such conditions are particularly true in the case of H_2O vapor. As the heat conductivity is further dependent on temperature (see Fig. 1.8b), it is evident that heat conductivity sensors require both temperature and humidity

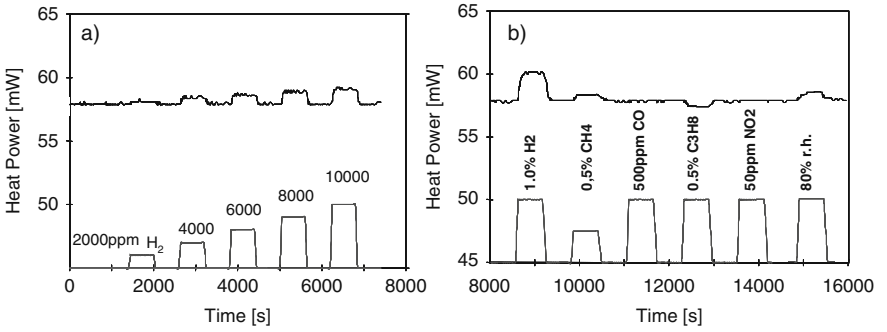

Fig. 1.9 (**a**) Output signal of a heated-membrane-type sensor in response to increasing concentrations of H_2; (**b**) Response of a heat conductivity sensor towards a range of gases that might interfere with H_2 detection

compensation in order to be useful. Discrimination of several gases becomes possible employing sensor array concepts [59].

Turning to the second application, namely vacuum pressure sensors, Fig. 1.8 shows that this is possible at pressures at which the mean free path becomes constrained by the dimensions of the micro-heater device. In the example considered in Fig. 1.7 we assumed that the distance between the heated membrane and the package is on the order of a typical silicon wafer thickness ($L_{wall} \sim 300$ μm). Such macroscopic air gaps can also be realized without invoking MEMS technologies. Macroscopic versions of heat conductivity sensors are currently in wide-spread use in the field of vacuum technology and they are well known under the name of Pirani gauges [70]. Making use of MEMS technologies and realizing very small gaps in the order of 1 μm or less between the heated membrane and a neighboring cold wall, the condition of geometrically constrained mean free paths can already be met in the range of normal ambient pressures [71, 72]. MEMS thermal conductivity sensors therefore can also be used for measurements in the meteorologically relevant range of air pressures. For such sensors all the above considerations concerning cross-sensitivity are relevant. As in a meteorological measurement the ambient temperature and the humidity are being measured alongside with the air pressure, temperature, and humidity compensation are of no concern in this particular application.

1.3.2 Metal-Oxide-Based Gas Sensors

The thermal conductivity sensors discussed above are physical sensors in the sense in that there is no chemical reaction at the heated membrane surface that leads to the detection reaction. A true chemical detection is enabled in case the heated membranes are fitted with gas-sensitive semiconductor materials,

which generate electrical output signals once chemical reactions are initiated at their surface. Very popular sensing materials are MOX semiconductors such as SnO_2, TiO_2, and WO_3 [13, 14, 15]. These materials are wide-band-gap semiconductors, which respond to changes in their gaseous environment via reversible conductivity changes [11, 12, 15, 16]. A common property of all these detection reactions is that they require significant levels of thermal activation to proceed at a measurable rate [73, 74]. In this context the heated-membrane device takes on the role of a thermal actuator, which simply supplies the heat that is necessary to initiate surface reactions at a chemically sensitive layer.

To date most commercial MOX gas sensors are prepared by means of screen printing onto bulk ceramic substrates [13, 14]. Due to their bulky nature, ceramic heater substrates consume heating powers on the order of 0.5–1 W per sensor element for attaining the required operation temperatures of about 400°C. This high level of power consumption represents a severe drawback when MOX gas sensors are to be used in bus-connected sensor networks or when sensor arrays with higher levels of gas discrimination are to be realized.

In order to improve this situation, a lot of research has been performed to arrive at much lower-power-consumption devices. This research has involved both the development of low-power-consumption heater devices as well as MOX deposition technologies that are compatible with these much more fragile micro-heaters [75, 76, 77, 78, 79, 80, 81, 82]. With regard to micro-heaters, most of the previous research had been dedicated to dielectric membrane-type devices [45, 46, 47, 48]. In contrast, most of our recent work was devoted to SOI-based heater technologies [28, 49, 50, 54, 55]. This move was largely motivated by the desire to gain processing stability on the level of the silicon MEMS technology as well as by providing substrates with higher mechanical stability and post-processing capabilities that allow innovative sensing layer technologies to be combined with micro-heater technologies [75, 76, 77, 78, 79, 80, 81, 82, 83, 84, 85, 86]. We will come back to this subject in Chapter 5 where we discuss such technologies with a special focus on industrialization aspects.

The SOI-based micro-heater devices developed in our lab are shown in Fig. 1.10 [28, 49, 50]. The top SOI layer in these array heater devices is shaped into thin silicon bridges that are suspended within a rigid chip frame. The heater current is passed directly through the heavily doped top silicon (Si:B) layer, which is about 6 μm thick (Fig. 1.10a). Due to the good thermal insulation, the center regions of the bridges can be heated to typical sensor operation temperatures of about 400°C by electrical power inputs of about 50 mW. On these center regions high-temperature stable and catalytically inactive SnO_2:Sb contacts have been formed to provide electrical access to the sensitive layers [57]. In order to enable different kinds of gases to be distinguished, the left-hand-side bridges carry pure tin dioxide (SnO_2) and the right-hand-side ones Pt-catalyzed SnO_2 gas-sensing layer (see Fig. 1.10b). The data in Fig. 1.11 show that the first